Acta Cryst. (1983). B**39**, 49–53

Electron-Density Distribution in Crystals of Potassium Tetrachloroplatinate(II) and Influence of X-ray Diffuse Scattering

By Shigeru Ohba,* Shoichi Sato and Yoshihiko Saito*

The Institute for Solid State Physics, The University of Tokyo, Roppongi-7, Minato-ku, Tokyo 106, *Japan*

and Ken-ichi Ohshima and Jimpei Harada

Department of Applied Physics, Nagoya University, Chikusa-ku, Nagoya 464, *Japan*

(*Received* 9 *June* 1982; *accepted* 8 *September* 1982)

Abstract

Charge-density distribution in crystals of $K_2[PtCl_4]$ has been determined by the X-ray diffraction method using Ag *Kα* radiation. The final *R* factor was 0·008 for 301 independent reflections ($\sin\theta/\lambda \leq 0{\cdot}8$ Å^{-1}). In the difference synthesis a trough of $-0{\cdot}4$ (1) e Å^{-3} was found on the Pt—Cl bond axis at 0·8 Å from the Pt nucleus, suggesting aspherical distribution of 5*d* electrons in the square-planar ligand field. A neutron diffraction experiment was also carried out, the final *R* factor being 0·039 for 169 independent reflections. The Pt—Cl bond distance determined by the X-ray analysis was 2·310 (1) Å, in good agreement with the 2·309 (1) Å obtained by the neutron study. The influence of diffuse scattering was detected on high-angle X-ray reflections. Not only thermal diffuse scattering but also some extra diffuse scattering, presumably due to some lattice defects, were shown to be present. [Crystal data: $K_2[PtCl_4]$, M_r = 415·1, tetragonal, *P*4/*mmm*, *a* = 7·024 (1), *c* = 4·147 (1) Å, *V* = 204·57 (2) Å^3, *Z* = 1, *T* = 297 K, D_x = 3·37 Mg m^{-3}, μ(Ag *Kα*) = 10·90 mm^{-1}.]

Introduction

Aspherical *d*-electron distribution around transition-metal atoms surrounded octahedrally or tetrahedrally by neighboring atoms has been studied by the X-ray diffraction method (Saito, 1979). The present study concerns a square-planar ligand field. Crystals of $K_2[PtCl_4]$ are built up of K^+ ions and square-planar $[PtCl_4]^{2-}$ complexes, as shown in Fig. 1 (Dickinson, 1922). The Pt and K atoms lie on special positions in the tetragonal lattice, and the Cl atom has only one variable positional parameter (see Table 3). Mais, Owston & Wood (1972) determined the structures of $K_2[PtCl_4]$ and $K_2[PdCl_4]$ with improved accuracy in order to determine accurate interatomic distances. It is worthwhile to see whether it is possible to observe charge asphericity around such a heavy atom as $_{78}$Pt. The contribution of valence electrons to the total X-ray intensities is very small so the intensities must be measured with high accuracy.

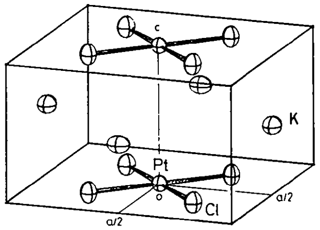

Fig. 1. Crystal structure of $K_2[PtCl_4]$ with atomic thermal ellipsoids scaled at the 50% probability level (Johnson, 1965). The thermal parameters obtained by the X-ray study are used.

Experimental

X-ray structure analysis

Crystals grown from an aqueous solution were ruby-red prisms elongated along the *c* axis. A crystal was shaped into a sphere of diameter 0·210 (2) mm with a piece of wet filter paper. Unit-cell dimensions were determined by a least-squares refinement with 15 independent 2θ values in the range $40 < 2\theta < 48°$, measured on a diffractometer using Ag *Kα* radiation (λ = 0·5608 Å). Crystal data are listed in the *Abstract*; Table 1 lists the experimental conditions. Intensity measurements were carried out on a Rigaku-3 automated four-circle diffractometer. Ag *Kα* radiation was used with a spherical specimen in order to reduce the systematic error caused by the absorption effect. The data collection was carried out up to 100° for 2θ with the θ–2θ scan technique. Eight equivalent reflections

---

* Present address: Department of Chemistry, Faculty of Science and Technology, Keio University, 3-14-1 Hiyoshi, Kohoku-ku, Yokohama 223, Japan.

0567-7408/83/010049-05$01.50

Table 1. *Experimental conditions for the X-ray intensity measurements*

Diameter of crystal specimen	0·210 (2) mm
Radiation	Ag $K\alpha$ (λ = 0·5608 Å)
Monochromator	Graphite plate
Collimator	0·5 mm ∅
Detector aperture	4·5 mm ∅ (0·94°; $2\theta \leq 60°$) 5·5 mm ∅ (1·15°; $60 < 2\theta \leq 100°$)
$(\sin\theta/\lambda)_{\max}$ of the observed reflections	1·37 $Å^{-1}$
Scan mode	θ–2θ scan
Scan speed	2° min^{-1} in θ ($2\theta \leq 60°$) 1° min^{-1} ($60 < 2\theta \leq 80°$) 0·5° min^{-1} ($80 < 2\theta \leq 100°$)
Scan width	(1·3 + tan θ)°
Maximum number of repetitions	2
Number of equivalent data measured for each reflection	8 ($2\theta \leq 60°$) 4 ($60 < 2\theta \leq 100°$)
Number of relections measured	6928
Number of non-zero reflections	6163
Number of independent reflections	1207

Table 2. *Observed and calculated structure factors of 00l reflections before and after the TDS correction*

				TDS corrected			TDS not corrected		
h	k	l	$\sin\theta/\lambda$ ($Å^{-1}$)	$\|F_o\|$	$\|F_c\|$	$\|F_o\|/\|F_c\|$	$\|F_o\|$	$\|F_c\|$	$\|F_o\|/\|F_c\|$
0	0	1	0·12	97·31	96·82	1·01	97·29	97·86	0·99
0	0	2	0·24	117·83	117·18	1·01	118·87	119·06	1·00
0	0	3	0·36	50·36	51·84	0·97	52·32	53·33	0·98
0	0	4	0·48	54·50	54·41	1·00	57·62	57·21	1·01
0	0	5	0·60	22·95	22·32	1·03	24·89	24·13	1·03
0	0	6	0·72	21·60	21·56	1·00	24·16	24·21	1·00
0	0	7	0·84	7·59	7·87	0·96	8·83	9·23	0·96
0	0	8	0·96	6·93	7·00	0·99	8·75	8·64	1·01
0	0	9	1·09	2·66	2·46	1·08	3·60	3·22	1·12
0	0	10	1·21	2·28	1·92	1·19	3·32	2·68	1·24
R*					0·020			0·025	
R_w					0·022			0·025	

* R values are for all the 1207 observed independent reflections.

were measured in the range $2\theta \leq 60°$, and four in the range $60 < 2\theta \leq 100°$. Internal agreement factors ($\sum\|\|F\| - \langle\|F\|\rangle\|/\sum\|F\|$) were 0·020 and 0·013, respectively, for all the observed 6163 reflections and 3272 reflections with $2\theta \leq 60°$. The crystal showed little anisotropy in the secondary-extinction effect. A total of 1323 independent reflections were measured and 1207 non-zero reflections were obtained and used for structure analysis.

Lorentz, polarization and absorption corrections with $\mu r = 1\cdot 14$ (Dwiggins, 1975) have been applied. The absorption-correction factor for $\|F_o\|$ was in the range 1·97 to 2·22. Parameters were refined by the full-matrix least-squares program *RADIEL* (Coppens, Guru Row, Leung, Stevens, Becker & Yang, 1979). The function minimized was $R_w = (\sum w\|\|F_o\| - \|F_c\|\|^2/\sum w\|F_o\|^2)^{1/2}$ with the use of the weight factor defined by $w^{-1} = [\sigma(\|F_o\|)]^2 + (0\cdot 015\|F_o\|)^2$. Valence form factors ($\kappa$) were introduced for Pt and Cl. The valence electrons of the Pt and Cl atoms were assumed to be $(5s)^2(5p)^6(5d)^8$ and $(3p)^6$, respectively and the atomic form factors for K^+ and Cl^- given by Fukamachi (1971) were used. The scattering factors of Pt were calculated from the Hartree–Fock wave-functions (Mann, 1967) using a program provided by Professor S. Wakoh of the University of Library and Information, Tokyo. Anomalous-dispersion corrections were taken from *International Tables for X-ray Crystallography* (1974).

It was found that $\|F_o\|$ of high-angle reflections was generally greater than $\|F_c\|$. In Table 2 the observed and calculated structure factors are compared for the 00l reflections. Good agreement between $\|F_o\|$ and $\|F_c\|$ is found from 001 to 008, $\Delta\|F\|$ being less than 4%; fairly large disagreement can be seen for 009 and 0,0,10. Fig. 2 shows the section of the difference synthesis through the $[PtCl_4]^{2-}$ plane. A sharp positive peak of 8·7 e $Å^{-3}$ appears at the origin, where the Pt atom is located, and this is surrounded by concentric spherical fringes. This anomaly may be a result of X-ray diffuse scattering, as will be discussed later. The elastic constants of $K_2[PtCl_4]$ crystals were determined by the ultrasonic pulse superposition method (Ohba, Matsuda, Hatta & Harada, 1981), with which the thermal diffuse scattering (TDS) was corrected by the program *TDS*2 (Stevens, 1974). The largest TDS correction factor was 0·637 for $\|F(0,4,11)\|$. After TDS correction, the R factor was reduced to 0·020 from 0·025 for 1207 independent reflections. However, the agreement between $\|F_o\|$ and $\|F_c\|$ was not improved sufficiently. Such disagreement seems to arise from the existence of extra diffuse scattering (EDS) under the Bragg reflections. The influence of EDS on the reflection data is considered to increase more rapidly with $\sin\theta/\lambda$ than for TDS. Since no method to correct such scattering caused by lattice defects has yet been established, higher-order reflections ($\sin\theta/\lambda >$ 0·8 $Å^{-1}$) were simply excluded from the present

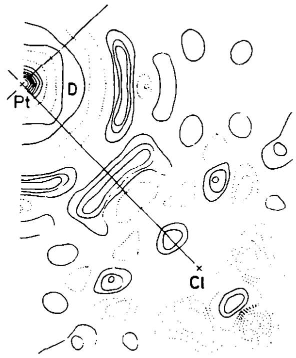

Fig. 2. Section of the difference synthesis through the plane of $[PtCl_4]^{2-}$ before TDS correction. Contours are at every 0·2 e $Å^{-3}$. In the vicinity of the Pt nucleus they are drawn at intervals of 1·0 e $Å^{-3}$. Negative contours are dotted.

refinement. Atomic positional and thermal parameters did not change significantly even if these reflections were excluded. When the population parameter of the valence orbitals of Pt was refined, the atomic charge of Pt exceeded +2. The atomic charges of Pt and Cl were then fixed to the values of Pt^{2+} and Cl^-, respectively. Since an extinction effect was noticed in the data, an isotropic-extinction correction (Zachariasen, 1967) was applied. The smallest extinction factor (F_o^2/F_c^2) was 0·54 for 100. The final R factor ($\sum||F_o| - |F_c||/\sum|F_o|$) was 0·008 and R_w = 0·011 for 301 independent reflections.* The valence form factors (κ) for Pt and Cl were 1·24 (1) and 1·11 (2), respectively. The positional parameter of the Cl atom was found to be x = 0·2325 (1), the Pt—Cl bond distance being 2·310 (1) Å.

Neutron diffraction study

Neutron diffraction measurements were also carried out in order to confirm the positional parameter of the Cl atom obtained by the X-ray study and to determine accurate thermal parameters. A crystal of $K_2[PtCl_4]$ grown from an aqueous solution in a desiccator containing sulfuric acid was ground into an approximate sphere of diameter 6·2 mm. Neutron diffraction measurements were performed on a four-circle diffractometer at the Research Reactor Institute, Kyoto University. The wavelength of the neutrons was 1·008 Å using a Cu monochromator. It was confirmed that ω-scan and θ–2θ-scan techniques gave the same integrated intensities as well as peak half-widths for 800 (2θ = 70·1°) and 201 (2θ = 22·1°). A typical peak half-width was 0·5° in θ. The intensity measurements were carried out up to a 2θ value of 100° for 317 reflections with the ω step-scan technique, and 266 (169 independent) reflection data were obtained. Two symmetry-related reflections were measured for 90 reflections which have relatively strong intensities. Their internal agreement factor was 0·013.

Intensity data were corrected for Lorentz, absorption (μr = 0·13) and TDS effects. Parameters were refined by the program *RADIEL*, where the weight was assigned as $w^{-1} = [\sigma(|F_o|)]^2 + (0{\cdot}015|F_o|)^2$. The function minimized was $R_w = (\sum w||F_o| - |F_c||^2/\sum w|F_o|^2)^{1/2}$. The scattering lengths (in fm) were taken from *International Tables for X-ray Crystallography* (1974): Pt 9·5, Cl 9·58, K 3·7. The scattering lengths were also refined in the final stage but no significant deviation was obtained. An isotropic-extinction correction was also applied to the neutron data. The smallest extinction factor (F_o^2/F_c^2) was 0·66 for 220. The final R factor ($\sum||F_o| - |F_c||/\sum|F_o|$) was 0·039 and R_w = 0·044 for 169 independent reflections.†

Measurement of X-ray diffuse scattering

Influence of X-ray diffuse scattering was noticed in high-angle reflections, and its effect on the difference synthesis was found to be serious. The intensity distribution of X-ray diffuse scattering around some reciprocal-lattice points was then measured to confirm its contamination in $|F_o|$'s.

The intensity of the X-ray diffuse scattering was measured using a four-circle diffractometer equipped with a Cu rotating-target X-ray generator (50 kV, 100 mA), a doubly bent LiF monochromator, a Ni—Co balanced filter and a pulse-height analyzer. Under the condition of symmetrical reflection from the (100) surface of an as-grown crystal of dimensions 5 × 8 × 10 mm, the intensity profiles along the circles, as illustrated in Fig. 3, were observed around the (400) reciprocal-lattice point with three different radii, $\frac{1}{9}a^*$, $\frac{1}{8}a^*$ and $\frac{1}{7}a^*$. The results are shown in Fig. 4, where the intensities are normalized in the direction N in the AC plane. The intensity of the TDS in the same direction from the reciprocal-lattice point falls off as the inverse square of the distance between the observation point and the reciprocal point. The profile along the circle with different radii must coincide with each other if there will be only TDS. The solid lines in Fig. 4 show the calculated TDS intensity based on the elastic-constant data (Wooster, 1962). As seen from Fig. 4, considerable extra diffuse scattering is found in the BC plane; in the AB and AC planes this is very strong in the directions B, B' and C, C'. The EDS forms a discoid in reciprocal space, whose normal is parallel to the a^* direction. There exists weak EDS in the directions of A and A'. This was assigned as Huang scattering due to long-range lattice strain from defect centers in the crystals because it does not appear in the direction perpendicular to the radial direction through the reciprocal-lattice point and the intensity is proportional to the inverse square of the distance from the reciprocal-lattice point. Such Huang scattering was

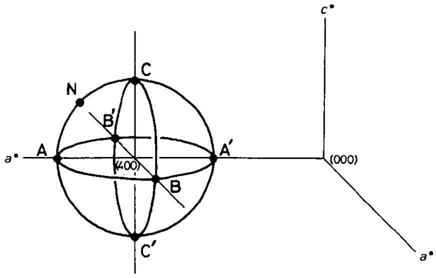

Fig. 3. Representation of three circles around the (400) reciprocal-lattice point, along which X-ray diffuse scattering was measured.

---

* Lists of structure factors from the X-ray and neutron diffraction studies have been deposited with the British Library Lending Division as Supplementary Publication No. SUP 38126 (14 pp.). Copies may be obtained through The Executive Secretary, International Union of Crystallography, 5 Abbey Square, Chester CH1 2HU, England.

† See deposition footnote.

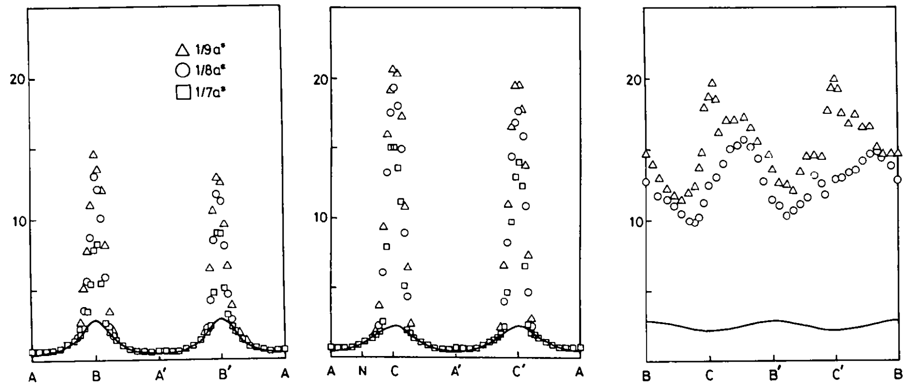

(a) (b) (c)

Fig. 4. Observed intensity profiles of the X-ray diffuse scattering around the (400) reciprocal-lattice point along the circles illustrated in Fig. 3. Solid curves show the theoretical intensity of TDS calculated with the elastic constants.

also observed around (401) and (220) reciprocal-lattice points.

Results and discussion

Charge asphericity

A difference synthesis was calculated using the reflection data with $\sin\theta/\lambda \le 0{\cdot}8$ Å^{-1}, where the subtracted densities were calculated on the basis of spherical atoms with charges K^+, Pt^{2+} and Cl^- using the refined radial parameters. In the calculation of the X–X synthesis the thermal parameters obtained by conventional refinement based on all the reflections with $\sin\theta/\lambda \le 0{\cdot}8$ Å^{-1} were used in order to avoid the effect of EDS. An attempt to carry out an X–N synthesis was given up, because the thermal parameters obtained by the neutron diffraction study were all greater than those from the X-ray study and this fact could not be rationalized (see Table 3). Fig. 5 shows a section of the X–X synthesis through the plane of $[PtCl_4]^{2-}$. A negative peak of $-0{\cdot}4$ (1) e Å^{-3} (marked by A) appears on the Pt–Cl bond axis at 0·8 Å from the Pt nucleus. It is theoretically expected that this peak is due to the deficiency in the $d_{x^2-y^2}$ orbital electron of the Pt atom. The energy level of the d orbital in a square-planar (D_{4h}) ligand field splits into the three singlets a_{1g}, b_{1g} and b_{2g} and the doublet e_g. The highest energy level among them is $b_{1g}(d_{x^2-y^2})$, the lobe of this orbital being directed toward the neighboring four Cl atoms. Then, eight $5d$ electrons of the Pt^{2+} ion occupy all the orbitals except $d_{x^2-y^2}$. On the Pt–Cl bond axis a positive peak (B) of 0·3 (1) e Å^{-3} is located at 1·2 Å from the Pt nucleus. Besides, there is a negative density (C) around the Cl nucleus. It is possible to assign these features as the polarization of spherical electron density around the Cl nucleus caused by formation of the coordination bond with the Pt^{2+} ion.

Peak heights in the difference synthesis are plotted against the cut-off value in Fig. 6. Peaks A and B are found to remain even for low cut-off values. On the other hand, an additional positive peak D, located on the bisector of angle Cl–Pt–Cl and at 0·42 Å from the Pt nucleus, appears for $(\sin\theta/\lambda)_{\max} = 1{\cdot}0$ Å^{-1}. Peak D is part of the fringes, which appeared in Fig. 2. This peak is negligible with low-angle reflections and it appears in the difference synthesis when higher-order reflections are included even after TDS correction. Such contamination of the difference synthesis is presumably related to the existence of EDS. It must therefore be remembered that high-angle reflections improve resolving power of the difference synthesis but sometimes give rise to spurious peaks. The present study, however, indicates that the detection of the

Table 3. *Positional and thermal parameters before and after the correction for thermal diffuse scattering*

Pt at (000)
4 Cl at $(x,x,0)$; $(x,-x,0)$; $(-x,x,0)$; $(-x,-x,0)$
2 K at $(0,\frac{1}{2},\frac{1}{2})$; $(0,-\frac{1}{2},\frac{1}{2})$; $(\frac{1}{2},0,\frac{1}{2})$; $(-\frac{1}{2},0,\frac{1}{2})$

	TDS corrected		TDS not corrected		X-ray (Mais, Owston & Wood, 1972)
	Neutron	X-ray	Neutron	X-ray	
Pt U_{11}	0·0269 (7)	0·0204 (1)	0·0228 (6)	0·0178 (1)	0·0180 (1)
U_{33}	0·0306 (13)	0·0234 (1)	0·0265 (11)	0·0206 (1)	0·0206 (1)
Cl x	0·2323 (1)	0·2325 (1)	0·2324 (1)	0·2325 (1)	0·2325 (1)
U_{11}	0·0315 (5)	0·0259 (1)	0·0276 (4)	0·0232 (1)	0·0242 (2)
U_{33}	0·0468 (8)	0·0421 (2)	0·0424 (6)	0·0393 (3)	0·0401 (5)
U_{12}	0·0026 (5)	−0·0030 (1)	−0·0028 (4)	−0·0030 (2)	−0·0057 (6)
K U_{11}	0·0552 (31)	0·0474 (4)	0·0520 (27)	0·0448 (5)	0·0451 (8)
U_{22}	0·0355 (24)	0·0326 (3)	0·0310 (20)	0·0301 (3)	0·0313 (6)
U_{33}	0·0357 (22)	0·0284 (2)	0·0309 (19)	0·0256 (3)	0·0261 (5)

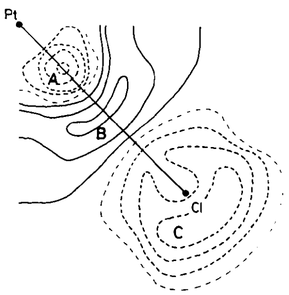

Fig. 5. Section of the difference synthesis through the plane of $[PtCl_4]^{2-}$ after TDS correction with cut-off value $(\sin\theta/\lambda)_{\max} = 0{\cdot}8$ Å^{-1}. Contours are drawn at intervals of 0·1 e Å^{-3}. Negative contours are broken, zero being chain-dotted.

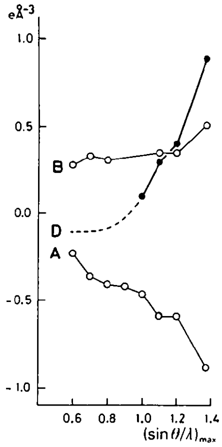

Fig. 6. Peak height of the deformation density in the difference synthesis as a function of the cut-off value, $(\sin\theta/\lambda)_{max}$ (Å^{-1}). Peaks *A* and *B* are as in Fig. 5 and *D* as in Fig. 2.

asphericity of 5*d* electrons is promising, if appropriate care is taken in experimental procedure.

Effective atomic charge of Pt

The number of electrons in a sphere centered on the Pt atom was calculated by direct integration of the observed electron density using all the observed X-ray reflection data (Sakurai, 1967), where the effect of series termination was corrected (Kobayashi, Marumo & Saito, 1972). A minimum of the radial distribution of charge density was found at 1·2 Å from the Pt nucleus, which is the distance between the Pt nucleus and the Pt—Cl bonding peak (*B*) shown in Fig. 5. Thus the radius of the Pt atom was assigned as 1·2 Å. The number of electrons in the sphere around Pt calculated before and after TDS correction was 77·2 (2) and 76·8 (2), respectively. Furthermore, when the $|F_c|$'s of high-order reflections ($\sin\theta/\lambda \geq 0{\cdot}8$ Å^{-1}) were used instead of the $|F_o|$'s to avoid the effect of EDS, this value became 77·0 (2). This result indicates that the effect of diffuse scattering on the direct integration is not serious. When the radius of the Pt atom was increased from 1·2 to 1·3 Å, the number of electrons increased from 77·0 (2) to 77·1 (2). Thus the effective charge of the Pt atom may be safely assigned to be +1. This qualitatively agrees with other experimental results. By pure quadrupole resonance of $_{35}$Cl (Marram, McNiff & Ragle, 1963) and by infrared reflection spectra (Hiraishi & Tamura, 1977), the effective ionic charge of the Pt atom in $K_2[PtCl_4]$ crystals was estimated to be +0·44 and +0·5, respectively.

Comparison between X-ray and neutron diffraction studies

In order to show the influence of TDS on the structure analysis, positional and thermal parameters obtained from the neutron diffraction data as well as from the X-ray intensity data before and after TDS correction are listed in Table 3. The parameters determined by Mais, Owston & Wood (1972) by the use of Mo *Kα* radiation are also compared in Table 3. They agree well with the values of the present X-ray study within 5*σ* before TDS correction. The thermal parameters increased by 6–19% after TDS correction. The thermal parameters obtained by the neutron diffraction study are greater than those obtained by the X-ray study by 10–30%. This discrepancy cannot be rationalized at present. The positional parameter of the Cl atom is not affected by TDS in agreement with the prediction given by Harada & Sakata (1974). The positional parameter obtained by the neutron diffraction method agrees well with that of the X-ray study. This means that there is no shift of the positional parameter of the Cl atom from the X-ray analysis due to the aspherical charge density around the Cl nucleus caused by the coordination bond with Pt^{2+}. A shift of the positional parameters of the first-row atoms toward the lone pair has been detected by combined X-ray and neutron diffraction studies (Coppens, 1974). Valence electrons of the Cl atom contribute to the total X-ray intensities to a relatively small extent because there are many core electrons, so that its charge asphericity may not affect the positional parameter.

Part of this work has been performed at the Research Reactor Institute, Kyoto University. The calculations were carried out on FACOM 230-48 and FACOM M-160F computers of the Institute for Solid State Physics, The University of Tokyo.

References

COPPENS, P. (1974). *Acta Cryst.* **B30**, 255–261.
COPPENS, P., GURU ROW, T. N., LEUNG, P., STEVENS, E. D., BECKER, P. J. & YANG, Y. W. (1979). *Acta Cryst.* **A35**, 63–72.
DICKINSON, R. G. (1922). *J. Am. Chem. Soc.* **44**, 2404–2411.
DWIGGINS, C. W. JR (1975). *Acta Cryst.* **A31**, 395–396.
FUKAMACHI, T. (1971). Tech. Rep. B12. Inst. for Solid State Physics, Univ. of Tokyo.
HARADA, J. & SAKATA, M. (1974). *Acta Cryst.* **A30**, 77–82.
HIRAISHI, J. & TAMURA, T. (1977). *J. Chem. Phys.* **66**, 3899–3902.
International Tables for X-ray Crystallography (1974). Vol. IV. Birmingham: Kynoch Press.
JOHNSON, C. K. (1965). *ORTEP*. Report ORNL-3794. Oak Ridge National Laboratory, Tennessee.
KOBAYASHI, A., MARUMO, F. & SAITO, Y. (1972). *Acta Cryst.* **B28**, 2709–2715.
MAIS, R. H. B., OWSTON, P. G. & WOOD, A. M. (1972). *Acta Cryst.* **B28**, 393–399.
MANN, J. B. (1967). *Atomic Structure Calculations* I. Report LA-3690. Los Alamos Scientific Laboratory, Univ. of California.
MARRAM, E. P., MCNIFF, E. J. & RAGLE, J. L. (1963). *J. Phys. Chem.* **67**, 1719.
OHBA, S., MATSUDA, T., HATTA, I. & HARADA, J. (1981). *J. Phys. Soc. Jpn*, **50**, 861–865.
SAITO, Y. (1979). *Inorganic Molecular Dissymmetry*, pp. 89–115. Berlin: Springer-Verlag.
SAKURAI, T. (1967). *X-ray Crystal Structure Analysis*, pp. 219–220. Tokyo: Shokabo.
STEVENS, E. D. (1974). *Acta Cryst.* **A30**, 184–189.
WOOSTER, W. A. (1962). *Diffuse X-ray Reflections from Crystals*, p. 74. Oxford Univ. Press.
ZACHARIASEN, W. H. (1967). *Acta Cryst.* **23**, 558–564.